Cross Validation to Select Material Models with Bulge Inflation Tests on PVC-coated Polyester

C. F. Jekel & R. T. Haftka
Department of Mechanical & Aerospace Engineering
University of Florida, Gainesville, FL, USA.

M. P. Venter & G. Venter
Department of Mechanical and Mechatronic Engineering
Stellenbosch University, Stellenbosch, South Africa.

ABSTRACT: Selecting an appropriate material model to generalize complex material behavior can be a difficult task, as there are many different formulations to choose from in commercial finite element (FE) programs. Four bulge inflation tests were performed on a PVC-coated polyester material with equivalently rated warp and fill strengths. Digital image correlation (DIC) was used to capture the full displacement field of the material at various pressure increments. An inverse analysis was set up to find material parameters in a FE model that matched the full displacement field of the experimental test. Cross validation was performed to investigate whether the physical behavior was better represented by an isotropic or orthotropic material model. This involved leaving out one of the four tests at a time. The orthotropic material model resulted in an average absolute deviation on the full displacement field that was 0.5% better than the isotropic model.

1 INTRODUCTION

The finite element (FE) method has become an important design tool for membrane structures, but it can be challenging to select the most appropriate material model for structural membrane materials. This is especially true for the most complex and non-linear materials including coated woven fabrics. Inverse analyses, or iterative schemes for FE model updating (FEMU) have been used to find material parameters from complex load cases. This paper proposes the use of cross validation to help select appropriate material models when using an inverse analysis (or FEMU) to determine parameters. Here, cross validation is used to select whether an isotropic or orthotropic material model is more appropriate for PVC-coated polyester characterized with a bulge inflation test.

PVC-coated polyester is a coated textile. It's most commonly modeled as an orthotropic material (Shaw et al. 2010), which is largely dependent on the warp to fill strength ratio (Dinh et al. 2017). Various non-linear models have been used in an attempt to better describe the behavior of the material. This has included a non-linear load ratio model (Galliot and Luchsinger 2009) and other non-linear orthotropic models (Ambroziak and Kłosowski 2014, Jekel et al. 2017).

Biaxial tests are commonly used to characterize material parameters for structural membrane materials (Stranghöner et al. 2016). Bulge (or bubble inflation) tests are a popular methodology to induce an equal biaxial load on the material. These bulge tests typically involve inducing a pressure on one side of a circularly clamped membrane material (Rachik et al. 2001, Charalambides et al. 2002, Machado et al. 2012, Tonge et al. 2013). The measured pressure and displacements are then used to infer material parameters.

Digital image correlation (DIC) is a non-invasive deformation measuring technique that has been used in a variety of applications (Becker et al. 2012, Murienne and Nguyen 2016, Mejía and Lantsoght 2016). The technique uses the correlation between consecutive images to calculate a full 3D displacement field. For bulge tests, DIC is an ideal tool to obtain a full 3D displacement field while not interfering with the inflation or deflection of the membrane material.

Material parameters in various models have been identified using FEMU (Lovato et al. 1993, Cailletaud and Pilvin 1994, Drass and Schneider 2016). The process can be generalized by using optimization to find parameters in a FE model to match some experimental behavior. In a forward problem parameters can be directly inferred from an experimental test. While an

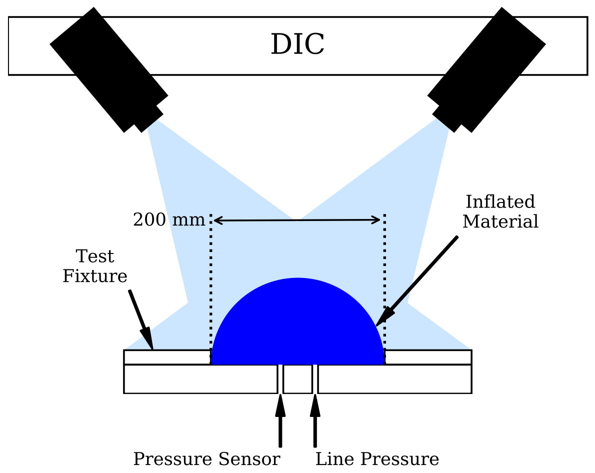

Figure 1: Bulge inflation test overview.

inverse problem attempts to tweak a model (like with FEMU) to find parameters that resemble an experimental response.

Four bulge inflation tests were performed on PVC-coated polyester. A FE model was constructed to replicate the physical conditions of the test. Inverse analyses were set up to determine isotropic and orthotropic material parameters by matching the FE model to the full displacement field of the bulge tests. Cross validation was then used to determine which material model had a better generalization of the experimental responses.

2 METHODS

An online repository is available at `https://github.com/cjekel/inv_bubble_opt` which includes the source code to perform the inverse analysis.

2.1 *Experimental tests*

The bulge inflation tests involve clamping a sample of membrane material into a circular clamp. Pressure is then induced on one side of the material. Displacements were measured using DIC of the material while simultaneously recording the inflation pressure. The DIC system used was the StrainMaster with DaVis (LaVision GmbH 2014). A visual annotation of the bulge inflation test setup is provided in Figure 1.

Four bulge inflation tests were performed. The PVC-coated polyester tested was Mehler Texnologies VALMEX® 7318. This material has a warp and fill tensile strength of about 3000 N/50 mm, a mass of 1000 g per square meter, and a thickness of 0.81 mm. Since the warp and fill strength from the manufacturer are equivalent, it might seem reasonable to investigate an isotropic material model. However, an isotropic material model would ignore the influence of the weave. Each test was inflated from zero to three bar.

Table 1: Number of unique (x, y, p) data points from each test and inflation pressures.

Test	# of data points	# of pressures
1	1,836,961	49
2	729,718	7
3	1,201,509	36
4	788,702	29

The bulge inflation tests using DIC resulted in a lot of generated data as shown in Table 1. The xy-plane coincided with the surface of the material prior to inflation, and the material was inflated in the z direction. The DIC system tracks the full displacement field of the bulge as it deforms. Each test resulted in approximately one million data points, where each data point represents a unique combination of inflation pressure p and initial x, y location. The deformation of each data point is represented as $\Delta x, \Delta y$, and Δz.

2.2 *Finite Element model*

An implicit non-linear FE model was constructed in ABAQUS to resemble the physical boundary conditions of the bulge inflation test. While there are analytical solutions to bulge inflation tests for isotropic and orthotropic material models (Sheplak and Dugundji 1998), it's desirable to use a FE model for designing other complex geometries. The model uses adaptive time stepping, and outputs the displacement fields at 201 pressure load steps between zero and three bar.

Linear isotropic and orthotropic material models were investigated. The isotropic model consists of two unknown parameters: the stiffness modulus (E) and the shear modulus (G). The orthotropic model was simplified as a three parameter model with a constant Poisson's ratio of 0.24. Jekel et al. (2016) showed that an orthotropic FE model of a bulge test was insensitive to Poisson's ratio. Using a constant Poisson's ratio simplifies issues with gradient magnitudes, as it's expected the gradient of Poisson's ratio will always be less than the stiffness moduli. The three unknown parameters in the simplified orthotropic model are the stiffness moduli (E_1 & E_2), and the shear modulus (G_{12}).

The displacement field of the FE model for an orthotropic material model at 2.0 bar is shown in Figures 2-4. Radial Basis Functions (RBF) are used to interpolate the displacements from the initial (x, y) node locations at each outputted pressure. The RBFs are exact at the node locations, and result in a smooth displacement field from the linear four node FE elements. The code available online contains an object to construct these RBFs to the full displacement field of the FE analysis using the SciPy *rbf* function (Jones et al. a).

Linear interpolation was used to evaluate the FE model's displacement in between the exported pressures, rather than exporting the node locations at the exact test pressures. The rational for this choice was that the FE model could be constructed independent

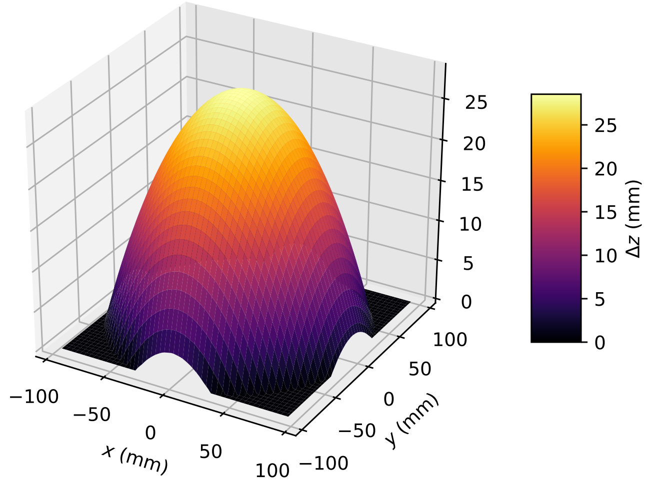

Figure 2: Displacement Δz of FE model at 2.0 bar.

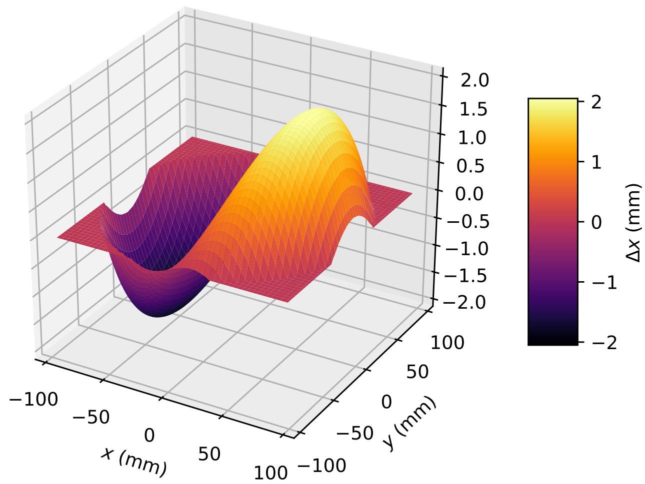

Figure 3: Displacement Δx of FE model at 2.0 bar.

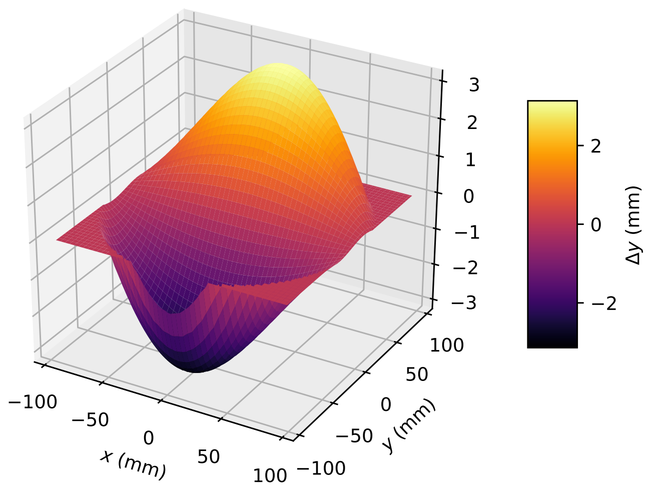

Figure 4: Displacement Δy of FE model at 2.0 bar.

of the test data. This allows for additional tests to be conducted and used in the inverse analysis without modifying the FE model's load increments. Linear interpolation is use to solve the displacement field $\Delta(x, y, p)$ by interpolating the displacement field at the two nearest pressures as

$$\frac{\Delta(x,y,p) - \Delta(x,y,p_1)}{p - p_1} = \frac{\Delta(x,y,p_2) - \Delta(x,y,p_1)}{p_2 - p_1} \tag{1}$$

where p_2 and p_1 represent the nearest pressures of the FE models' load steps.

2.3 *Inverse analysis*

Optimization is used to find the material model parameters which minimize the discrepancy between the physical bulge inflation tests and the FE model. This discrepancy is formulated as the average $L1$ distance in mm as

$$e(\boldsymbol{\beta}) = \sum_{j}^{n_t} \frac{r_{\Delta x}(j, \boldsymbol{\beta}) + r_{\Delta y}(j, \boldsymbol{\beta}) + r_{\Delta z}(j, \boldsymbol{\beta})}{n_t} \tag{2}$$

where n_t is the total number of tests. The average absolute deviation between the x displacement of the FE model and inflation test is denoted $r_{\Delta x}(j, \boldsymbol{\beta})$ for the j test and $\boldsymbol{\beta}$ set of material parameters. These average absolute deviations are expressed as

$$r_{\Delta x}(j, \boldsymbol{\beta}) = \sum_{i=1}^{n_j} \frac{|\Delta x(x_i, y_i, p_i)_t - \Delta x(x_i, y_i, p_i, \boldsymbol{\beta})_f|}{n} \tag{3}$$

$$r_{\Delta y}(j, \boldsymbol{\beta}) = \sum_{i=1}^{n_j} \frac{|\Delta y(x_i, y_i, p_i)_t - \Delta y(x_i, y_i, p_i, \boldsymbol{\beta})_f|}{n} \tag{4}$$

$$r_{\Delta z}(j, \boldsymbol{\beta}) = \sum_{i=1}^{n_j} \frac{|\Delta z(x_i, y_i, p_i)_t - \Delta z(x_i, y_i, p_i, \boldsymbol{\beta})_f|}{n} \tag{5}$$

where n_j is the total number of data points in the j test. The subscripts t is for the physical inflation test data, while the subscript f is from the FE model.

The optimization problem is then stated as

$$\text{minimize:} \quad e(\boldsymbol{\beta}) \tag{6}$$

$$\text{subject to:} \quad \beta_l \leq \beta_k \leq \beta_u, \quad k = 1, 2, \cdots, n_p. \tag{7}$$

where $\boldsymbol{\beta}$ is the vector of material parameters which are restricted to some reasonable lower and upper bounds. The isotropic parameters are expressed as $\boldsymbol{\beta} = (E, G)$, and the simplified orthotropic parameters are expressed as $\boldsymbol{\beta} = (E_1, E_2, G_{12})$.

The optimization strategy used involved first starting with a global optimizer with an allocated number of function evaluations. When the global optimizer reached the limit of function evaluations, a local optimizer was used to polish the result. The global optimization strategy used was Efficient Global Optimization (EGO), which utilized the expected improvement from a Gaussian process to minimize the function (Jones et al. 1998, The GPyOpt authors 2016). A variant of the BFGS (Broyden 1970, Fletcher 1970, Goldfarb 1970, Shanno 1970) gradient based optimization was used as the local optimizer (Jones et al. b, Byrd et al. 1995). Initially 50 EGO function evaluations (calculations of e) were performed before switching to the BFGS implementation. A budget of 200 function evaluations for the BFGS appeared to be sufficient at finding a local optimum.

There is the possibility that some combination of material parameters may cause the FE analysis to not converge. This is problematic when the optimization algorithm requires a discrepancy for a particular set of parameters that are unable to converge. To deal with this problem, the maximum objective value from the run-time history was passed to the optimization algorithm when the FE analysis failed to converge. Additionally, a discrepancy value of 30 mm was passed if the first function evaluation in a given run failed to converge. This strategy works well with EGO, however it creates a non-differentiable objective function which can be problematic for gradient based optimization algorithms. Looking at the optimization history, the FE analysis would only fail to converge during the line search stage of the gradient based optimization algorithm, and not the finite differences which approximate the gradients. This is less problematic because the gradients were accurate, however caution should be expressed when utilizing this strategy with gradient based optimization algorithms.

2.4 *Cross validation*

Cross validation is a model selection or validation tool used in various regression problems to assess the quality of models(Queipo et al. 2005). Cross validation provides for a nearly unbiased estimate of the modeling error, and can be used to diagnose overfitting or bias errors. Cross validation can be used to compare the performance of one material model to another in the context of fitting material models with an inverse analysis (FEMU). This may be important in practice when the ideal material model is unknown. In this case, cross validation will be used to quantitatively compare how the linear isotropic and orthotropic material models represent the behavior of PVC-coated polyester from these bulge inflation tests.

The processes proposed is similar to leave-one-out cross validation, and is described as:

1. Perform inverse analysis without test j
2. Calculate the discrepancy e on the left-out test j
3. Repeat 1 & 2 for all tests
4. The cross validation score is the average discrepancy e from the left-out tests

This cross validation score was computed for both the linear isotropic and orthotropic material models. The model with the lower cross validation score is assumed to be a better generalized representation of the material behavior.

3 RESULTS

Inverse analyses were performed to fit isotropic and orthotropic material models to the bulge inflation tests. Additional inverse analyses were performed such that a leave-one-test-out cross validation score was computed for each material model. The resulting discrepancy values are presented in Table 2. The orthotropic material model had lower discrepancy and cross validation scores. This result implies that the orthotropic material model was a better representation of the physical bulge inflation test than the isotropic material model. While the orthotropic material model was better, the difference between the cross validation scores was only 0.5%.

Table 2: Resulting discrepancy from the inverse analysis and leave-one-test-out cross validation.

		Cross Validation	
Model	e (mm)	e_{CV} (mm)	Range of e
isotropic	1.763	1.927	0.708
orthotropic	1.757	1.918	0.672

The isotropic material model parameters from the full inverse analysis and the cross validation runs are presented in Table 3. The stiffness modulus varied from 0.155 to 0.198 GPa, and the shear modulus varied from 0.052 to 0.070 GPa. The orthotropic material model results are shown in Table 4. There was more variance on the E_1 modulus (0.228 to 0.312 GPa) than the E_2 modulus (0.232 to 0.246 GPa). Leaving test 1 out resulted in the most different material parameters for both material models.

It's interesting to evaluate the discrepancy from each set of material parameters on the various cross validation test configurations. This was done in Table 5 for the isotropic material model, and Table 6 for the orthotropic material model. A row in the table represents all of the discrepancy values from that set of material parameters. The abbreviation CV1 represents the cross validation from leaving test 1 out, and full represents the results from using all of the tests.

Table 3: Resulting isotropic material parameters from each inverse analysis. Note ν_{12} calculated from E and G.

	GPa		
	E	G	ν_{12}
All test data	0.166	0.055	0.509
Leaving test 1 out	0.155	0.052	0.490
Leaving test 2 out	0.193	0.067	0.440
Leaving test 3 out	0.167	0.056	0.491
Leaving test 4 out	0.198	0.070	0.286

Table 4: Resulting orthotropic material parameters from each inverse analysis.

	GPa		
	E_1	E_2	G_{12}
All test data	0.264	0.246	0.003
Leaving test 1 out	0.228	0.240	0.003
Leaving test 2 out	0.312	0.235	0.005
Leaving test 3 out	0.300	0.232	0.005
Leaving test 4 out	0.280	0.244	0.003

Table 5: Objective values from each isotropic material parameter set.

	Objective value e (mm)				
	Full	CV1	CV2	CV3	CV4
Material Full	1.76	1.72	1.74	1.77	1.82
Material CV1	1.82	1.65	1.86	1.84	1.92
Material CV2	1.80	1.84	1.72	1.80	1.84
Material CV3	1.76	1.73	1.74	1.77	1.82
Material CV4	1.79	1.79	1.74	1.79	1.84

For each optimization to be successful, the minimum in any given column should occur from the row of the same name. Again for both the isotropic and orthotropic results it appears that leaving test 1 out resulted in the most different objective functions.

4 DISCUSSION

The difference between the isotropic and orthotropic material models was only 0.5% based on the cross validation score of the discrepancy function. The difference being only 0.5% was an interesting outcome, because an orthotropic material model is favored for this material and it was expected to perform much better than the isotropic material. Perhaps the inclusion of Poisson's ratio as a parameter in the orthotropic model would result in an improved material model. Again, cross validation scores could be used to evaluate whether the orthotropic model benefits from the additional parameter. If computational budget is a concern, it should be cheaper to optimize the two parameter isotropic model as oppose to the orthotropic model.

Leaving test 1 out resulted in the most different material parameters and discrepancy values. This implies that test 1 may be the most different of the other tests. It may be interesting to fit material parameters to each test individually, to see if the parameters from test 1 result in an outlier. The tests were conducted at different inflation rates, so it was not entirely unexpected that individual test may result in different material parameters. The various inflation rates from each test may have activated different non-linear material behavior.

Table 6: Objective values from each orthotropic material parameter set.

	Objective value e (mm)				
	Full	CV1	CV2	CV3	CV4
Material Full	1.76	1.72	1.73	1.77	1.81
Material CV1	1.81	1.64	1.85	1.83	1.90
Material CV2	1.78	1.82	1.71	1.77	1.81
Material CV3	1.76	1.76	1.72	1.77	1.81
Material CV4	1.76	1.75	1.72	1.77	1.80

For the orthotropic material when considering all bulge tests, sets $(E_1 = 0.264, E_2 = 0.246, G_{12} = 0.003)$, $(E_1 = 0.300, E_2 = 0.232, G_{12} = 0.005)$, and $(E_1 = 0.280, E_2 = 0.244, G_{12} = 0.003)$ all produce a discrepancy value of 1.76 mm to three digits. It's possible that the objective function was relatively flat in this domain, since the discrepancy varied little between these material parameter sets.

5 CONCLUSION

An inverse analysis was proposed to find material parameters by matching the full displacement from bulge inflation tests on PVC-coated polyester. Optimization was used to find the material parameters in a FE model that best matched the DIC experimental displacement field. Cross validation was used to select whether an isotropic or orthotropic material model was a better representation of the PVC-coated polyester in the bulge tests. The orthotropic material model had a better cross validation score, and was concluded as being a better representation of the PVC-coated polyester. However, the cross validation discrepancy value was only 0.5% better than the isotropic material model.

Cross validation as a model selection tool can be used to identify overfitting, while also providing a more realistic discrepancy in a potential sampling bias. While overfitting is not much of a concern with the large amount of data and few material parameters, more complex and non-linear material models may overfit the test data. In this study, the cross validation indicates that the discrepancy was about 10% worse than it appears due to sampling bias.

ACKNOWLEDGMENTS

Thanks to Sudharshan Udhayakumar for help constructing the FE model and comparing the FE model to analytical solutions. Thanks to Andrés Bernardo for helping set up script to process the full displacement field data. Charles F. Jekel has received the following funding for his PhD research which has supported this work: University of Florida Graduate Preeminence Award, U.S. Department of Veterans Affairs Educational Assistance, and Stellenbosch University Merritt Bursary.

REFERENCES

Ambroziak, A. & P. Kłosowski (2014, jan). Mechanical properties for preliminary design of structures made from PVC coated fabric. *Construction and Building Materials 50*, 74–81.

Becker, T. H., M. Mostafavi, R. B. Tait, & T. J. Marrow (2012). An approach to calculate the J-integral by digital image correlation displacement field measurement. *Fatigue & Fracture of Engineering Materials & Structures 35*(10), 971–984.

Broyden, C. G. (1970, mar). The Convergence of a Class of Double-rank Minimization Algorithms 1. General Considerations. *IMA Journal of Applied Mathematics 6*(1), 76–90.

Byrd, R. H., P. Lu, J. Nocedal, & C. Zhu (1995). A limited memory algorithm for bound constrained optimization. *SIAM Journal on Scientific Computing 16*(5), 1190–1208.

Cailletaud, G. & P. Pilvin (1994). Identification and inverse problems related to material behaviour. *Inverse problems in engineering mechanics 1*, 79–86.

Charalambides, M., L. Wanigasooriya, G. Williams, & S. Chakrabarti (2002, jan). Biaxial deformation of dough using the bubble inflation technique. I. Experimental. *Rheologica Acta 41*(6), 532–540.

Dinh, T. D., A. Rezaei, L. Daelemans, M. Mollaert, D. V. Hemelrijck, & W. V. Paepegem (2017). A hybrid micro-meso-scale unit cell model for homogenization of the nonlinear orthotropic material behavior of coated fabrics used in tensioned membrane structures. *Composite Structures 162*, 271–279.

Drass, M. & J. Schneider (2016). On the mechanical behavior of transparent structural silicone adhesive–TSSA. In *SEMC 2016–Sixth International Conference on Structural Engineering, Mechanics and Computation*, pp. 14–16.

Fletcher, R. (1970, jan). A new approach to variable metric algorithms. *The Computer Journal 13*(3), 317–322.

Galliot, C. & R. Luchsinger (2009). A simple model describing the non-linear biaxial tensile behaviour of PVC-coated polyester fabrics for use in finite element analysis. *Composite Structures 90*(4), 438–447.

Goldfarb, D. (1970). A family of variable-metric methods derived by variational means. *Math. Comp. 24 (1970), 23-26*.

Jekel, C. F., G. Venter, & M. P. Venter (2016). Obtaining a hyperelastic non-linear orthotropic material model via inverse bubble inflation analysis. *Structural and Multidisciplinary Optimization*, 1–9.

Jekel, C. F., G. Venter, & M. P. Venter (2017, feb). Modeling PVC-coated polyester as a hypoelastic non-linear orthotropic material. *Composite Structures 161*, 51–64.

Jones, D. R., M. Schonlau, & W. J. Welch (1998, dec). Efficient Global Optimization of Expensive Black-Box Functions. *Journal of Global Optimization 13*(4), 455–492.

Jones, E., T. Oliphant, P. Peterson, & Others. SciPy: Open source scientific tools for Python.

Jones, E., T. Oliphant, P. Peterson, & Others. {SciPy}: Open source scientific tools for {Python}.

LaVision GmbH (2014). *Product-Manual DaVis 8.2 Software* (8.2 ed.). Göttingen, Germany.

Lovato, G., F. Moret, P. Le Gallo, G. Cailletaud, & P. Pilvin (1993). Determination of brazed joint constitutive law by inverse method. *Le Journal de Physique IV 3*(C7), C7—-1135.

Machado, G., D. Favier, & G. Chagnon (2012). Membrane curvatures and stress-strain full fields of axisymmetric bulge tests from 3D-DIC measurements. Theory and validation on virtual and experimental results. *Experimental mechanics 52*(7), 865–880.

Mejía, C. A. & E. O. L. Lantsoght (2016). Strain and deflection analysis in plain concrete beams and reinforced concrete beams by applying Digital Image Correlation. In *SEMC 2016–Sixth International Conference on Structural Engineering, Mechanics and Computation*. CRC Press.

Murienne, B. J. & T. D. Nguyen (2016). A comparison of 2D and 3D digital image correlation for a membrane under inflation. *Optics and Lasers in Engineering 77*, 92–99.

Queipo, N. V., R. T. Haftka, W. Shyy, T. Goel, R. Vaidyanathan, & P. Kevin Tucker (2005, jan). Surrogate-based analysis and optimization. *Progress in Aerospace Sciences 41*(1), 1–28.

Rachik, M., F. Schmidtt, N. Reuge, Y. Le Maoult, & F. Abbeé (2001). Elastomer biaxial characterization using bubble inflation technique. II: Numerical investigation of some constitutive models. *Polymer Engineering & Science 41*(3), 532–541.

Shanno, D. F. (1970). Conditioning of quasi-Newton methods for function minimization. *Math. Comp. 24 (1970), 647-656*.

Shaw, A., S. Sriramula, P. D. Gosling, & M. K. Chryssanthopoulos (2010). A critical reliability evaluation of fibre reinforced composite materials based on probabilistic micro and macro-mechanical analysis. *Composites Part B: Engineering 41*(6), 446–453.

Sheplak, M. & J. Dugundji (1998, mar). Large Deflections of Clamped Circular Plates Under Initial Tension and Transitions to Membrane Behavior. *Journal of Applied Mechanics 65*(1), 107–115.

Stranghöner, N., J. Uhlemann, F. Bilginoglu, K.-U. Bletzinger, H. Bögner-Balz, E. Corne, N. Gibson, P. Gosling, R. Houtman, J. Llorens, & Others (2016). Prospect for European Guidance for the Structural Design of Tensile Membrane Structures. *Science and Policy Report (SaP-Report). Draft Version. To be published by the Joint Research Centre (JRC) of the European Commission, publication expected*.

The GPyOpt authors (2016). GPyOpt: A bayesian optimization framework in python. `http://github.com/SheffieldML/GPyOpt`.

Tonge, T. K., L. S. Atlan, L. M. Voo, & T. D. Nguyen (2013). Full-field bulge test for planar anisotropic tissues: Part I – Experimental methods applied to human skin tissue. *Acta Biomaterialia 9*(4), 5913–5925.